Monitoring small-strain stiffness and permeability of geomaterials for environmental use

Original
Monitoring small-strain stiffness and permeability of geomaterials for environmental use / Bernardo, D., Di Sante, M., Fratalocchi, E., Mazzieri, F.. - In: ENVIRONMENTAL GEOTECHNICS. - ISSN 2051-803X. - ELETTRONICO. - 13:5(2026), pp. 466-478. [10.1680/jenge.25.00079]

Availability:
This version is available at: 11566/354373 since: 2026-03-20T08:39:55Z

Publisher:

Published
DOI:10.1680/jenge.25.00079

Monitoring Small-Strain Stiffness And Permeability Of Geomaterials For Environmental Use

Author 1

- Davide Bernardo[1], PhD
- SpS Mobile, Ancona
- ORCID number

Author 2
- Marta Di Sante[2], PhD
- Associate Professor, Department SIMAU, Marche Technical University, Ancona Italy;
- 0000-0003-1216-3440

Author 3
- Evelina Fratalocchi, PhD
- Full Professor, Department SIMAU, Marche Technical University, Ancona, Italy
- 0000-0001-9162-2929

Author 4

- Francesco Mazzieri, PhD
- Associate Professor, Department SIMAU, Marche Technical University , Ancona, Italy
- 0000-0001-9815-4048

Full contact details of corresponding author.

Francesco Mazzieri, PhD,

Associate Professor, Department SIMAU, Marche Technical University, Via Brecce Bianche,12, Ancona 60131, Italy

e-mail:f.mazzieri@staff.univm.it

Abstract

Cement-bentonite (CB) mixtures, compacted soil-lime (SL), and compacted soil-lime-fly-ash (SLFA) mixtures are frequently used materials in environmental engineering. The properties of these materials change over time due to chemical reactions between the binder, soil, and/or water. The acceptance criteria for these materials are usually defined by specific property values, such as permeability, stiffness, and shear strength, measured at certain curing times. The small-strain shear modulus, G_0, can be non-destructively measured using the Bender Element (BE) method. The present paper illustrates the trend of G_0 in CB, SL, and SLFA mixtures over curing time until 60 to 90 days. In addition, the hydraulic conductivity, k, was also measured. Three different CB mixtures, one SL mixture, and one SLFA mixture were examined. It was observed that the G_0 for the CB mixtures increased as the curing time progressed, while the k decreased noticeably. The ratio of cement to water in CBs seemed to play a key role in determining the G_0, while other factors, like the use of additives, also significantly affected the k. For SL and SLFA mixtures, the G_0 was found to rise with curing time, showing a pattern reflecting the advancement of pozzolanic reactions between the soil and binders, and the permeability correspondingly decreased within one order of magnitude.

Keywords

Cement/cementitious materials, lime, fly ash, permeability, small-strain stiffness

List of notations

BE	Bender elements
α	CB permeability reduction coefficient
CB	Cement-Bentonite mixture
SLFA	Compacted Soil-Lime-Fly-Ash mixture
SL	Compacted Soil-Lime mixture
FA	Fly ash
f	Frequency of the transmitted wave
k_{ref}	Hydraulic conductivity at a reference time t_{ref},
OPC	Ordinary Portland Cement
t_{p-p}	Peak-to-peak travel time in BE testing

t_{ref} Reference time

f_R Resonant frequency of the BE-specimen system

k Saturated hydraulic conductivity

V_s Shear wave velocity

$G_{0,28d}$ Small-strain shear modulus at 28 days of curing

G_0 Small-strain shear modulus or small-strain stiffness

L_{tt} Tip-to-tip distance between the bender elements.

λ Wavelength of the transmitted signal

1. INTRODUCTION

Porous materials comprised of cement (e.g., water-cement-bentonite blends or "CB" mixtures, Jefferis, 1981) and soil modified by binders find frequently use in geo-environmental engineering. They are crucial in projects like cut-off walls, landfill sloping sidewalls (e.g., cement-soil mixture, Bellezza and Fratalocchi, 2006), and in the reutilisation and/or stabilization of excavated earth (e.g., soil-lime mixtures, TRB, 1987; Beetham et al., 2014; Di Sante et al., 2020). Beyond the customary cement-based and lime-based materials, the current requirements for sustainable geotechnical methods have pushed researchers to find solutions that incorporate industrial waste and byproducts. This has resulted in a rising interest in the exploration of soil improvement methods leveraging innovative and environmentally sound substances (Devi et al., 2020). Fly ash (FA) is one of these effective byproducts utilized to enhance soil characteristics (Noaman et al., 2022). FA is a material that exhibits pozzolanic properties; its function is greatly enhanced in an alkaline medium, meaning it's usually combined with soil in conjunction with an activating agent (e.g., sodium hydroxide or lime, Costa et al., 2023).

A shared feature of these materials is that some of their characteristics (like stiffness, shear strength, and water permeability) change over time due to pozzolanic reactions, even without any chemical interactions. In lab or field research, as well as during quality checks and assurance processes, it is important to consider how these properties change with time. This knowledge is useful for deciding when to conduct tests, evaluating how hydration reactions progress, and determining if the material meets the required standards at a specific time.

A mechanical factor that indicates the qualities of the porous material is the small-strain shear modulus, G_0. This parameter is related to the stiffness of the soil structure and is expected to change as pozzolanic reactions take place with curing time. Additionally, changes to the microscopic and macroscopic structure of the porous materials caused by chemicals (for instance, the formation of expansive ettringite and the cracking of cement materials when in the presence of dissolved sulphate anions) should be revealed through a change in G_0. In laboratory assessments, G_0 can be accurately measured without damaging the sample by using the Bender Elements (BE) technique, which allows the same sample to be tested throughout the entire curing stage.

BE testing has recently been applied to observe the increase in stiffness of porous cement-based materials made from various combinations of cement, lime, and fly ash. Verástegui Flores et al. (2013) monitored the small-strain shear modulus and hydraulic conductivity (k) of a CB specimen subjected to water or sodium sulfate permeation through BE tests. While permeating with water, G_0 increased, and k gradually reduced over time due to hydration of cement. Conversely, after extended exposure to sulphates, a decline in G_0 and a progressive rise in k were observed, indicating deterioration of the cementitious matrix, leading to a reduction in strength and the formation of a network of interconnected cracks that impacted the k. Li et al. (2019) employed BE to examine how curing times, type of cementitious material (which included Ordinary Portland Cement, OPC, and slag), and the rate of slag substitution influenced the shear wave velocity V_s of slag-cement-bentonite blends (S-CB). The findings revealed that V_s (along with G_0) for

S-CB increased with age and proportion of cementitious components while showing a decrease with higher slag substitution levels. Additionally, it was noted that the trend over time for the normalized modulus ($G_0/G_{0,28d}$), where $G_{0,28d}$ refers to the measurement taken at 28 days, was more influenced by the rate of slag substitution than by the overall amount of cementitious material.

Puppala et al. (2005) examined the G_0 of expansive clays that were treated with lime and cement for a deep mixing project. Puppala et al. (2006) observed the changes in stiffness of sulphate-rich soils treated with cement and lime through BE tests, and noted a considerable rise in G_0 with curing time, attributed to the addition of binders. Wang et al. (2017) developed an innovative approach to measure G_0 by comparing the received BE signals of shear waves (S-waves) and compressional waves (P-waves) and applied the developed method on a plastic silt treated with 2% quicklime. Verástegui Flores et al. (2010) employed BE testing and standard unconfined compression testing to track the progress of hardening in clay treated with cement over time. Their findings indicated that both G_0 and the strength of cement-treated samples increase logarithmically with time. For various cement types, both the G_0 and compressive strength were normalized with respect to values determined of 28 days, and a similar trend of increase was observed.

The small-strain shear modulus typically increases upon incorporation of FA into soil. Some studies have investigated soil-FA blends with various FA amounts and found that G_0, assessed through the BE test, increased with FA content and curing time (Ingale et al., 2019) particularly in case of addition of cement (Piriyakul, 2014; Petcherdchoo et al., 2023). Additional factors that enhance the small-strain stiffness in soil-FA blends include the confining pressure, relative compaction, and the frequency of the applied waveform (Ram and Mohanty, 2021). Notable increases in shear wave velocity were observed with further addition of polymers like Polyethylene Oxide and Chitosan to the soil-FA blend (Kang, 2015).

This paper summarizes selected findings from a current research program investigating the engineering characteristics of geomaterials utilized in environmental projects. Specifically, the paper focus is on employing the BE method to track the changes in the small-strain shear modulus of cement-bentonite (CB), soil-lime (SL) and soil-lime-fly ash (SLFA) mixtures. The primary aim was to establish an optimized testing approach for cement-based materials, adapted to the continuous evolution of the properties of concern over time. The following geo-materials were examined: a) three CB mixtures with varying formulations, reflecting a spectrum from low to high quality mixture; b) one SL mixture, incorporating a lime amount typically used in practice (3% quicklime); c) one SLFA combination that includes 2% fly ash (as the pozzolanic agent) and 2% lime (as the activating component). BE assessments were associated with permeability evaluations, either on the same specimen or on different ones, to jointly analyze the changes in hydraulic and stiffness characteristics. Lastly, scanning electron microscopy (SEM) analysis of the microstructure of the treated soils was conducted to further enhance the understanding of the experimental findings.

2. MATERIALS

2.1 Cement-bentonite (CB) mixtures

The study utilized two types of bentonites (one calcium: Ca-bentonite and one sodium: Na-bentonite), a simulated III/B type cement made of 30% OPC and 70% blast furnace slag and Ancona (Italy) tap water. A polymeric liquid additive (LAVIODIS®, Laviosa S.p.A, Italy) was incorporated into CB2 and CB3. The chemical composition of the additive is undisclosed. The only information available to the authors is that the additive is a liquid water-soluble dispersant based on a particular proprietary polymer. It appears as an orange-yellow liquid with a slight organic odour. According to the specification sheet of the product, the main function of the additive is to improve the workability and the stability of the mixture.

2.2 Soil-Lime (SL) mixture

A highly plastic inorganic clay (Liquid Limit=57%, Plasticity Index=33%, classified as group a clayey soil of high plasticity-CH in the Unified Soil classification System, ASTM D2487, 2017), denoted as MSC was used as the base for the soil-lime (SL) mixture (refer to Table 1). The lime utilized is a fine calcic quicklime, designated as CL80-Q (UNI EN 459-1, 2010), which entirely passes through the ASTM 200 sieve (75 μm opening).

Table 1. Main properties of the soils used in this study

Property	SGT soil	MSC soil
Sand (%) [a]	3	3
Fine (%)[a]	97	97
Clay (<2μm,%)[a]	39	52
Liquid limit (%)	40	57
Plasticity index (%)	20	33
ICL [b] – %CaO	2	1.5

[a] ASTM D422 (2014)

[b] ICL=initial consumption of lime (ASTM D6276, 2019)

2.3 Soil-lime-fly ash (SLFA) mixture

The soil for the soil-lime-fly ash (SLFA), identified as SGT, consists of clay of low plasticity (classified as clayey soil of low plasticity-CL group in the Unified Soil Classification System , ASTM D2487, 2017); the primary properties of both SGT and MSC soils are detailed in Table 2. The lime utilized is the same as that for the preparation of the SL mixture. The fly ash (FA) utilized is a highly pozzolanic product (provided by General Admixtures S.p.A., Italy). The unit weight of FA solids is 22 kN/m^3. When used in a SLFA composite, the lime function is the activator of the FA, which represents the pozzolanic precursor. Microstructural investigation and chemical analyses the FA (scanning electron microscopic, SEM, observations - Figure 1 and Energy Dispersive X-Ray Spectroscopy, EDS) allowed identifying the main elements (45% silicon, 23% aluminum 10% iron, 10% calcium, 4% potassium by weight, excluding oxygen). The mineralogical composition (by means X-Ray diffraction analyses) includes quartz, calcium oxide and mullite ($Al_{4.56}\,Si_{1.44}\,O_{9.72}$) as main components.

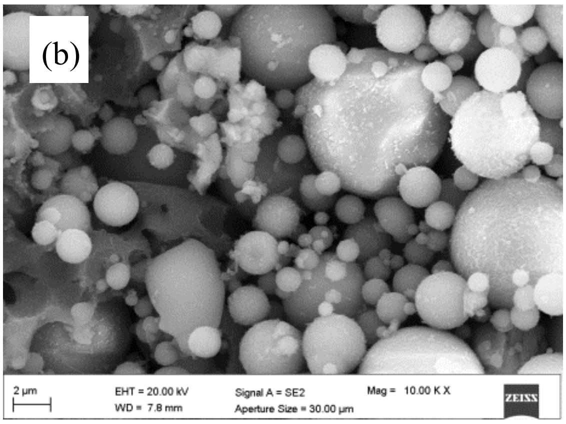

Figure 1. SEM image of the FA (Magnification:10000x)

3 METHODS

3.1 Sample preparation

The CB mixtures were prepared by dusting powdered bentonite into water (CB1) or into water pre-mixed with the additive (CB2 and CB3) using a high-speed shear mixer set at 1000 revolutions per minute (rpm) for 15 minutes. The bentonite slurry was left to fully hydrate for 24 hours. Subsequently, cement was incorporated into the bentonite slurry while agitating the slurry at a speed of 1500 rpm. Mixing was continued at the same speed for additional 5 minutes after ending the addition of cement. The quantity of mixture produced for each batch enabled the determination of Marsh viscosity, unit weight (γ), and bleeding. The freshly made mixtures were poured into cylindrical split plastic moulds of the same dimensions as the test specimens (diameter=10.0 cm, length=6.0 -7.0 cm). The moulds containing the test specimens were submerged in water to facilitate curing and to avoid drying out. After a minimum curing duration of 7 days, the hardened specimens were removed from the moulds for further testing.

The SL specimens were prepared with a lime rate of 3% of the soil dry mass. First, the air-dried soil was broken down, and moisture (tap water) was added until the target water content (26%). Lime was then mixed with the wet soil to achieve an even distribution. The resulting mixture was compacted in accordance with the Standard Proctor procedure (ASTM D698, 2021) in three separate layers. The sample used to assess G_0 had a void ratio of 0.74 and an initial saturation degree of 93%. The compacted specimens were kept in a sealed plastic container and placed at a controlled temperature of 22 ± 2°C, only removed briefly from the container for BE testing. To reduce water loss during the curing phase and the testing process, the specimens were fully coated in paraffin, leaving only the BE slots exposed, immediately after compaction. The specimen was repeatedly weighed throughout the curing duration, with evaporation resulting in a mass of under 1%. Following the same method (excluding the paraffin coating), another specimen was prepared for testing permeability.

The SLFA mixture was prepared by mixing the dry binders, using quantities equivalent to 2% of the dry weight of the soil for both lime and FA, and subsequently the binders with the soil previously moistened at target water content, *w,* of 20%. The resulting SLFA mixture was then compacted following the Standard Proctor as per ASTM D698 (2021). For the measurement of the G_0, a specimen with a void ratio of 0.5 and an initial saturation degree of 95% was selected. The BE testing was conducted under unconfined conditions. To prevent moisture loss, the specimen was covered with a latex membrane. A different specimen was prepared using the same method for testing the permeability.

3.2 BE apparatus and testing

BE testing was carried out in general accordance with the ASTM Standard D8295 (2019). A sine pulse signal with an amplitude of 10 V was produced using a function generator (Aim TTI TG5011A), which was triggered with a period that allowed sufficient time for the damping of the BE response prior to the subsequent pulse. The signals, both sent and received, were captured using a digital oscilloscope (Picoscope 6, Pico Technology LTD, UK). The time for shear wave travel was calculated using the time domain method (Peak-to-peak). Signals covering the frequency range from 0.5 kHz to 50 kHz were generated.

For testing CB mixtures, the slots for inserting the BE were obtained using a thin plastic sheet matching the size of the transducer; this sheet was pressed into the fresh, relatively soft mixture and removed before BE testing commenced. Care was taken to ensure that the slots on opposite sides of the samples were properly aligned. After a curing period of 7 days in water, the specimen was placed into a triaxial cell to apply a confining stress while keeping the saturation condition. The pedestal and top cap of triaxial cell are provided with BE (Controls, Italy). A confining effective stress of 35 kPa was applied to the specimen and maintained for the entire duration of the test. The BE testing took place at specified curing times.

The BE tests for the SL and SLFA mixtures was conducted on unconfined specimens, an approach frequently utilized for stabilized soils (e.g. Puppala et al., 2006; Tang et al., 2011; Wang et al., 2017; Wang et al., 2020). A narrow slot was cut shortly after compaction on the two opposite bases of the compacted cylindrical specimens to enable the insertion of the BE; care was taken to ensure proper alignment. To perform the measurement, the specimen was positioned horizontally on a custom-made wooden holder. The first measurement was taken two hours following the compaction of the sample and extraction from the mold; subsequent readings were taken at specified curing times up to 81 days.

3.3 Permeability tests

Concerning CB mixtures, *k*, was assessed using the same triaxial cell apparatus (i.e. flexible wall permeameter) by alternating permeation stages and BE testing. For SL and SLFA mixtures, the compacted samples were kept in sealed plastic bags until they were moved to flexible wall permeameters, within one week of curing. The specimens underwent consolidation under an isotropic effective stress of 35 kPa, and were permeated with tap water for a minimum of 28 days of curing. In the case of SL and SLFA mixtures, the consolidation phase is preceded by three saturation steps of 30 minutes each, in order to gradually increase the confining and the pore pressures to reach the selected effective stress. The 35kPa stress level was chosen to simulate the confinement conditions of BE testing, which occurred without confinement, while still ensuring proper contact between the specimen and the latex membrane. Tap water was selected as the permeating fluid rather than deionized or distilled water to reflect the typical operational conditions found at construction sites. Additionally, it is important to note that the presence of lime results in the porewater composition of lime-treated soils being primarily influenced by hydroxide dissociation and the resulting exchange of adsorbed cations for calcium. Hence, utilizing distilled or tap water as the permeating fluid should not lead to significant differences in the permeability of the materials. Following the *k* tests, Scanning Electron Microscope (SEM) analyses were conducted using VEGA3 – TESCAN (Czech Republic) and FESEMSUPRA40–ZEISS (Germany), after the samples underwent air dewatering and gilding by means of an Emitech K550 sputter coater.

4 RESULTS AND DISCUSSION

4.1 BE testing: signal interpretation

Figure 2 illustrates an example of results of BE measurement conducted on the CB mixture. The travel time was determined as the peak-to-peak time difference ($t_{p\text{-}p}$) between the input and received wave (Fig 2). The G_0 of the sample at the specified curing time was therefore calculated as:

$$G_0 = \rho \left(\frac{L_{tt}}{t_{p\_p}} \right)^2 \qquad (1)$$

where ρ= specimen density and L_{tt} =tip-to-tip distance between the BE elements. Multiple frequencies, f, of the emitted signal were systematically used to identify the clearest signal. For CB2, both the transmitted and received signals diminished in strength over time, complicating the determination of the travel time (Figure 2b). The specific cause of this phenomenon, likely linked to a defect in the electronics, was not identified. Nevertheless, the readable signals were considered.

For each measurements, the ratio of L_{tt} to the wavelength, λ (calculated as V_s/f), was consistently evaluated to ensure that $2 < L_{tt}/\lambda < 9$, thereby ensuring the output signal's clarity, meaning it was not masked by the dominance of the near-field effect (Sanchez Salinero et al., 1986; Arulnathan et al., 1998; Arroyo et al., 2003; Wang et al., 2007).

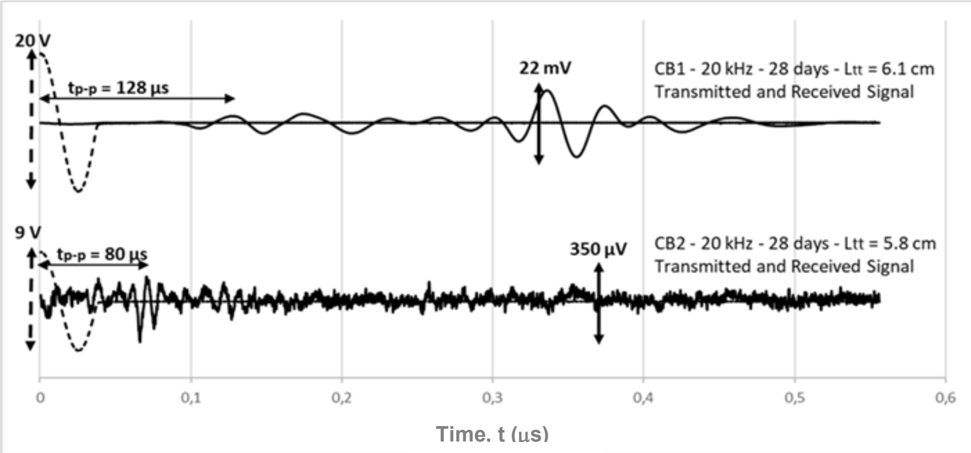

Figure 2. Examples or transmitted and received signals during BE testing of CB mixtures.

4.2 CB Mixtures

4.2.1 CB mixtures properties

Three different CB mixtures were prepared in this study. The main physical properties obtained for the three mixtures are detailed in Table 2.

Table 2. Main physical properties of the tested CB mixtures

Mixture	Bentonite		Cement	Additive	Marsh Funnel Test (ASTM D6910)	γ [b]	Bleeding (ASTM C232)
	Type	Amount	c/w[a]				
[-]	[-]	[g/l]	[-]	[%]	[s]	[[kN/m³]	[%]
CB1	Ca	65	0.27	-	35	11.6	6.5
CB2	Na	60	0.27	0.2	46	11.8	<1
CB3	Na	60	0.22	0.2	53	11.8	<1

[a]c/w=water-cement ratio ; [b] γ = unit weight

The cement-to-water ratio and the bentonite type were varied to evaluate their impact on the G_0 of the mixture. Since CB mixtures have been extensively studied (e.g. Fratalocchi et al., 2022), the impact of factors such as cement type, cement content, bentonite type etc. on their hydraulic and mechanical behaviour is well recognized. Therefore, the CB mixtures prepared in this study may be considered to encompass the possible range of behaviours expected in the field. In particular, CB1 aimed at representing a low-quality mixture (Ca-bentonite, no additive), while CB2 and CB3 simulated higher quality mixtures (Na-bentonite, with additive).

4.2.2 G_0 vs. curing time

In Figure 3, the G_0 modulus of the three CB mixtures considered in in this study is plotted for curing times ranging from 14 to 60 days. For CB2, only limited data are available due to the previously mentioned problems with weak signals. The G_0 values for all CB mixtures showed an increase with curing time, beyond the 28-day conventional period utilized for assessing the properties of cementitious materials. This growth in G_0 with curing times correlates with enhanced stiffness of the solid skeleton resulting from cement hydration products, such as C-S-H. The relationship between G_0 and curing time is well represented by a logarithmic law (Verástegui Flores et al., 2010), particularly for CB1 and CB3, as illustrated in Figure 2. The data for CB2 show greater variability but remain on average close to those for CB1. The main differences between CB1 and CB2 lie in the type of bentonite used and the inclusion of additives; however, both had identical quantities of cementitious materials (the sum of cement and slag), which seems to be the key factor in influencing the small strain stiffness of the CBs material under the specified testing conditions. Indeed, CB3 with a lower c/w ratio (c/w=0.22) compared to CB1 and CB2 (c/w=0.27) had significantly lower G_0 values.

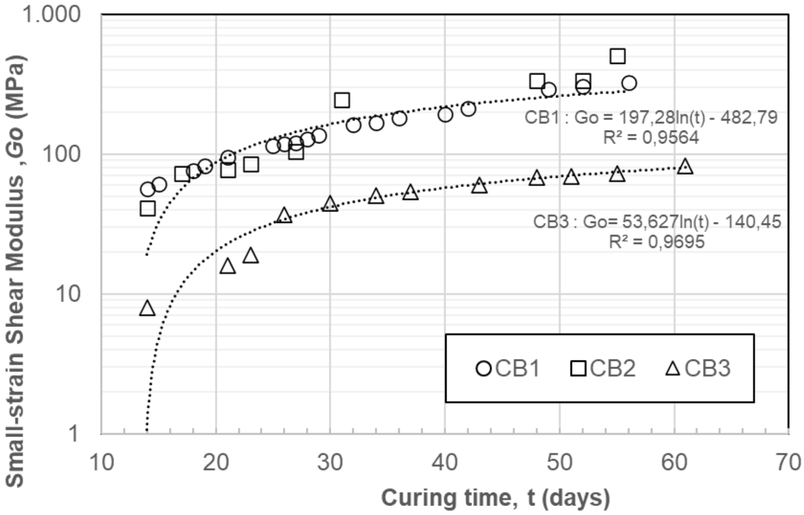

Figure 3. G_0 versus curing time for the CB mixtures investigated. Dotted lines are the best-fit curves of experimental data for CB 1 and CB 2

The G_0 values obtained in this study vary significantly from those documented in the literature concerning CB mixtures of comparable composition. For instance, Verástegui Flores and Di Emidio (2013) obtained $G_{0,28\,d}$ =150 MPa for a CB mixture consisting of 4% sodium bentonite, 16% III/B cement (containing 66-80% slag), and 80% water by weight. In this study $G_{0,28\,d}$= 38 MPa was obtained for CB3, which contains 5% sodium bentonite, 17% cementitious materials (70% slag), and 78% water by weight. Additionally, Li et al. (2019) reported $G_{0,28\,d}$ = 0.25 MPa for a CB mixture that comprised 15% cementitious material (30% OPC and 70% slag). The substantial variation in values across different investigations involving relatively similar mixtures of the same age implies that the measured G_0 of CB mixtures is profoundly influenced by the testing conditions (e.g., the stress state) and by the type and quality of the components used.

4.2.3 Hydraulic conductivity vs curing time

Figure 3 illustrates the (saturated) hydraulic conductivity of the three CB mixtures vs.

curing time (measured in days from when the mixtures were prepared) specifically during the curing period from 14 to 60 days. It is widely recognized that the *k* of CB mixtures declines over time due to of cement hydration (Fratalocchi and Pasqualini, 1998). The relationship between the saturated *k* of CB mixtures and the curing period, *t*, can be effectively represented by a power law model (Fratalocchi and Pasqualini, 1998; ICE, 1999):

$$k(t) = k_{ref}\left(\frac{t}{t_{ref}}\right)^{-\alpha} \qquad (2)$$

where $k_{ref} = k$ at a reference time, t_{ref}, and α = the *k* reduction coefficient.

The fitting parameters in Equation 2 tend to vary at shorter curing times but generally stabilize after approximately 40 to 60 days. In Figure 4, the experimental data of *k* vs curing time and the fitting curves based on Equation 2, (assuming t_{ref}=14 days) are shown. The resulting Equation for each mixture is also shown. Throughout the time frame examined, the *k* values for CB1 and CB2 differed by around two orders of magnitude. This difference primarily stems from the additive's influence and to some extent from the type of bentonite used, given that both mixtures had identical total cement content and a slag substitution rate of 70%. Despite the total porosity of the mixtures being nearly identical, the lower *k* value for CB1 can be attributed to differences in size and distribution of the conductive pores, likely influenced at the initial slurry phase by the effects of the additive and sodium bentonite, which contribute to a more dispersed arrangement of cement particles compared to CB2. Conversely, the α coefficients for CB1 and CB2 are quite similar, largely due to the cement-to-water ratio in both mixtures, which is the same (0.27). The observed difference in *k* between the two mixtures is expected to continue even with extended curing durations, as indicated by the *k*(*t*) Equations in Figure 3. While CB2 and CB3 display comparable k_{ref} values at t equals 14 days, their α values differ, which can be attributed to the varying cement-to-water ratios.

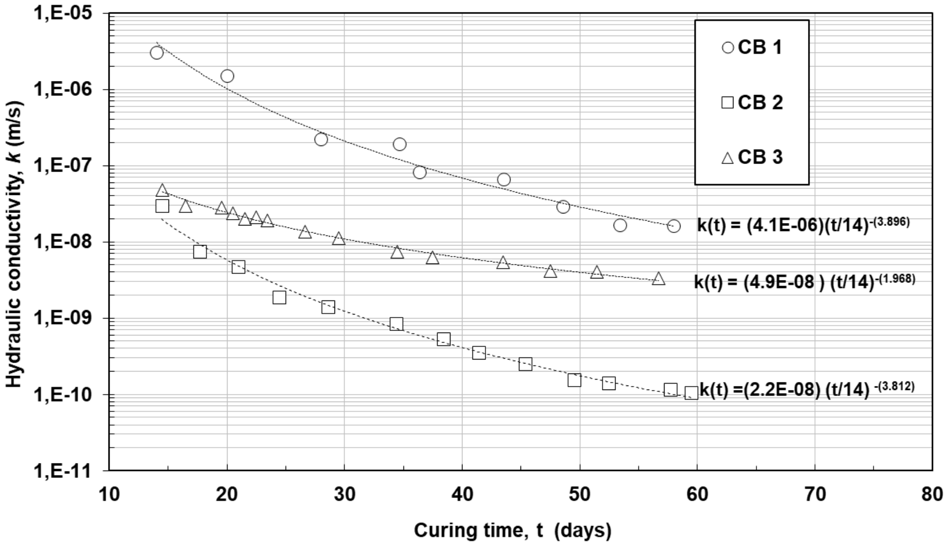

Figure 4. Hydraulic conductivity vs. curing time of the three CB mixtures investigated. Dotted lines are the best fit curve of experimental data according to Equation 2.

When analysing the results in Figure 3 and Figure 4, while CB1 and CB2 show comparable values of G_0, their k values vary significantly, differing by two orders of magnitude. As a result, establishing one single relationship between G_0, k, and curing time for CB mixtures is not feasible. Nevertheless, observing the G_0 of a specific CB mixture along with its permeability could offer a more thorough understanding of the material's behaviour, which is essential for design considerations. A notable variation from the anticipated pattern in G_0, such as an abrupt drop or an absence of increase at shorter curing times, could serve, along with k, as a signal or warning for inconsistencies in the properties of the mixture or in lab procedures. On the contrary, the present data indicated that, for a specific curing time, the G_0 values are greater for the CB mixture that has a higher ratio cement-to-water ratio. Thus, G_0 could be utilized as a marker for cement content in CB mixtures of equivalent age, for a given cement type.

4.3 SL and SLFA mixtures

4.3.1 G_0 versus curing time

The relationship between G_0 and curing time for lime-treated soil is illustrated in Figure 5. As expected, there is a growing trend with curing time, that can be effectively captured by a logarithmic function of time. The early curing phase (0-10 days) is zoomed in Figure 5. For the SL mixtures the starting G_0 value of 21 MPa corresponds to the compacted, untreated MSC soil. At t=2 days, G_0 showed a significant increase relative to untreated soil, reaching 679 MPa at 10 days of curing; thereafter, a more gradual increase was noted, with a maximum value of 1127 MPa at 81 days. This pattern primarily results from cation exchange, induced by the Ca^{2+} cations released from dissociation of calcium hydroxide, and the consequent immediate flocculation of soil particles, which accounts for the initial slight increase in stiffness relative to untreated soil during at early curing times (0-2 days).

The notable rise in G_0 after 2 days of curing (refer to the expanded graph) reflects the dominance of pozzolanic reactions compared to cation exchange. The increase in G_0 from 2 days to 81 days of curing can be attributed to the cementation processes in the sample, resulting from the ongoing pozzolanic reactions. The findings align with other research (for example, Wang et al. 2020; Liu et al. 2021) on lime-treated soils, where a two-phase increase pattern of the G_0 modulus was consistently observed. Additionally, the correlation between the G_0 trend and both short-term and long-term reactions between soil and lime has recently been reinforced by concurrent observation of porewater chemistry (Di Sante et al. 2022).

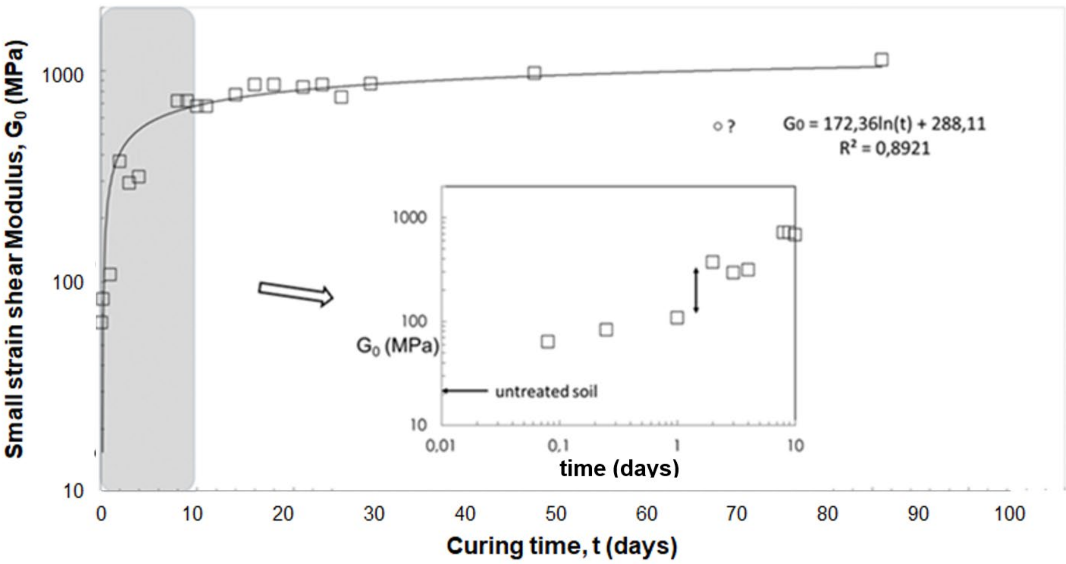

Figure 5. G_0 vs. curing time for the SL mixture investigated.

Investigating the behaviour of G_0 for the SLFA mixture with curing time (Figure 6), a clear upward trend of the parameter with curing time is evident. Moreover, a logarithmic relationship effectively represents the obtained experimental results (R^2=0.95). The early curing phase (0-10 days) is zoomed in Figure 6, where a rapid rise to 124 MPa shortly (1.5 hours) after compaction can be observed, assuming G_0 of the compacted untreated soil (15 MPa) as the initial point. Following the initial sharp increase, a more gradual increase to approximately 324 MPa was noted within 10 days of curing. Between 10 to 90 days, G_0 displayed minimal variation, maintaining a value of about 350 MPa at 90 days.

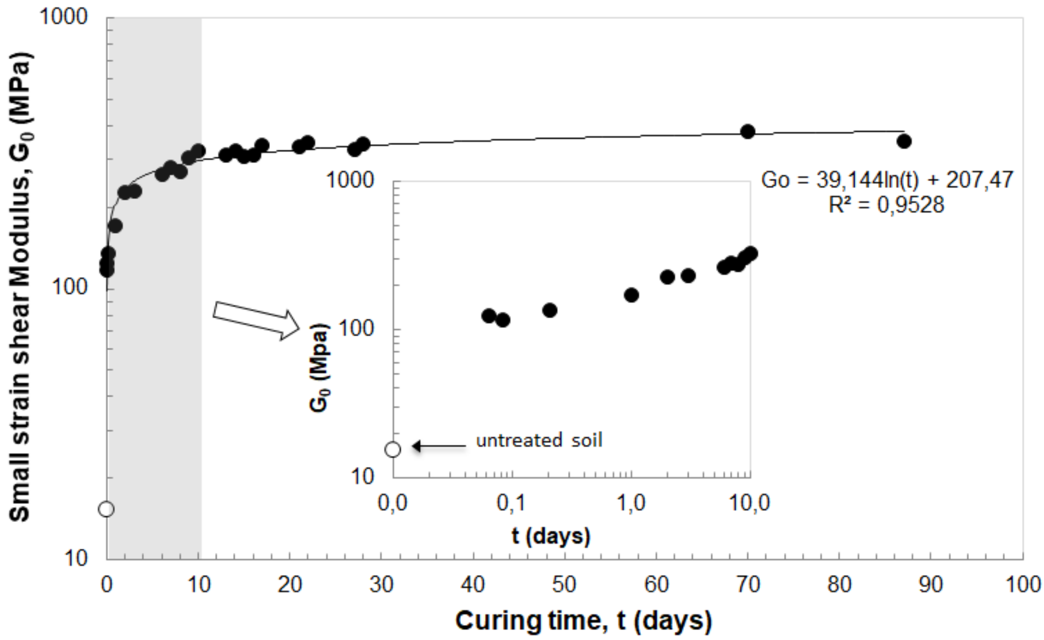

Figure 6. ***G_0* vs. curing time for the SLFA mixture investigated**.

To understand this trend, it is important to recognize that the rapid hydration of calcium oxide (quicklime), leads to the formation of calcium hydroxide, or hydrated lime. This process is subsequently followed by the dissociation of calcium hydroxide in porewater, resulting in both an increase in pH levels and interaction with the cations adsorbed on clay particle surfaces. In an alkaline setting, the reactivity of fly ash is maximized, prompting the rapid formation of pozzolanic compounds. Consequently, there is a notable and immediate rise in G_0, driven by both the aggregation of clay particles and the rapid generation of pozzolanic products. If the subsequent changes in G_0 are ascribed to the progression of pozzolanic reactions, it can be generally concluded that these reactions are completed within the first 10 days of curing.

A factor that can enhance the clarity of the signal during BE testing is the frequency of the emitted wave; specifically, changing the frequency led to a significant variation the ratio L_{tt}/λ. Furthermore, the ratio L_{tt}/λ diminished as the curing period increased for a specific frequency, which is consistent with the rise in stiffness (i.e., V_s) associated with curing. According to Lee and Santamarina (2005), the clarity of the signal received is maximized when the frequency of the transmitted wave closely matches the resonant frequency of the soil-BE system, noting that increased soil stiffness results in a higher resonant frequency, f_R. In this study, f_R was determined for both SL and SLFA mixtures using Lissajous forms, yielding the f_R values depicted in Figure 7, which are shown as a function of curing time. For both the SL and SLFA mixtures, the resonant frequency rises with the increase in curing time.

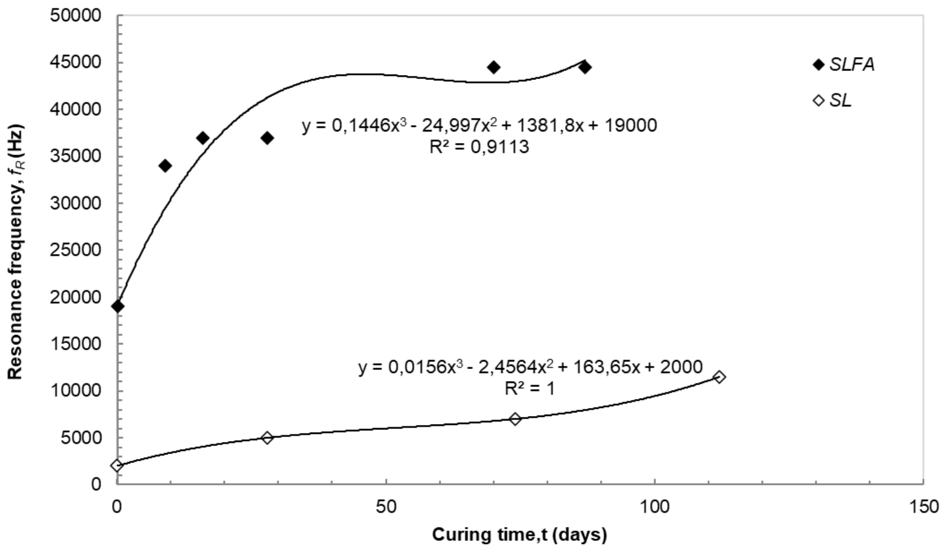

Figure 7 Resonance frequency f_R of the SL and SLFA specimens as a function of curing time

4.3.2 Hydraulic conductivity versus curing time

Figures 8 and 9 illustrate the hydraulic conductivity with curing time for the SL and SLFA mixtures, respectively. The k of the untreated compacted soil (measured on a different sample under similar confining pressure) is provided as a comparison for both materials. It can be noted that the inclusion of binders significantly increased k when compared to the untreated compacted soil. Specifically, for the SL mixture, the initial $k = 4\times10^{-7}$ m/s, showing an increase of over three orders of magnitude when compared to the untreated soil (k = 6-8$\times10^{-11}$ m/s). For the SLFA mixture, the k value after two days of curing was 9.2×10^{-8} m/s, whereas the untreated compacted soil had k value of 1.8×10^{-9} m/s. This rise in k is caused by dissociation of lime and the release of calcium cations into the pore water, promoting cation exchange and causing clay particles to agglomerate into larger clusters, thereby creating conductive pores among these aggregates (TRB, 1987).

For the SLFA mixture, the increase in k values relative to the untreated soil was less pronounced than that observed in the SL mixture, by roughly two orders of magnitude. This is likely attributable to two primary reasons: 1) the SGT soil contains a smaller clay content (refer to Table 1), which results in a higher k compared to the compacted untreated MSC soil; thus, the soil exhibits reduced sensitivity to cation exchange and flocculation following lime treatment; 2) the amount of lime used in the SLFA mixture is lower than that used in the SL mixture.

In the long term, a slight decrease in k was observed to 1×10^{-7} m/s for SL and to 1.3×10^{-8} m/s for the SLFA, respectively. The slow decline in k can be attributed to the formation of amorphous pozzolanic reaction products, that partially fill the inter-aggregate voids (Wild et al.,1987). In brief, the pattern of k during the curing interval examined essentially confirms the long-term development phase of soil-binder interactions suggested by the G_0 trend; particularly for the SLFA mixture, the most significant reduction takes place during the initial ten days of curing, consistently with the G_0 trend that was observed.

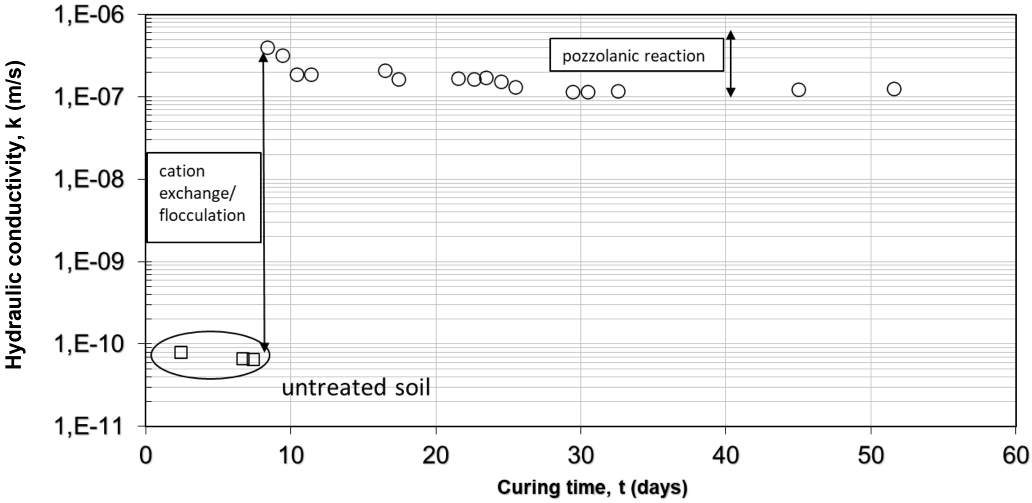

Figure 8. Hydraulic conductivity versus curing time for the SL mixtures investigated. The hydraulic conductivity of the compacted untreated soil is shown for comparison.

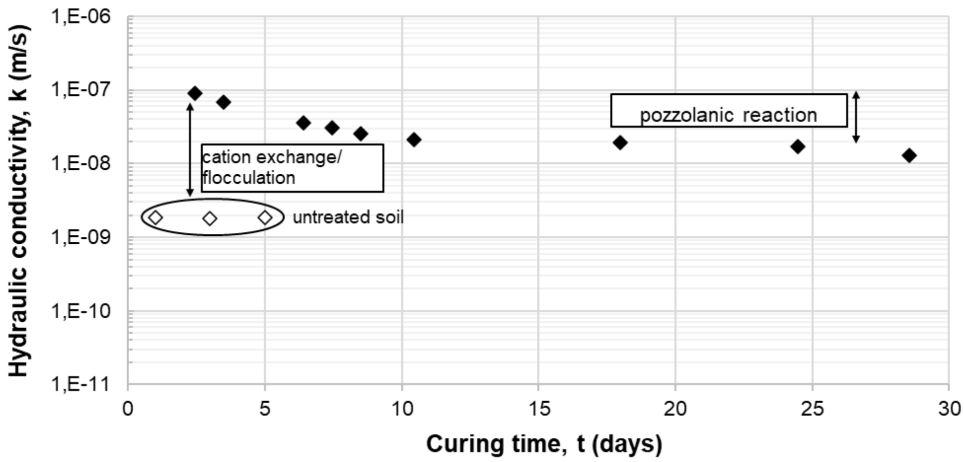

Figure 9. Hydraulic conductivity versus curing time for the SLFA mixtures investigated. The hydraulic conductivity of the compacted untreated soil is shown for comparison.

4.3.3 *Microstructural investigation*

In Figure 10, Scanning Electron Microscope images of both the untreated soil (Figure

10a) and the SL mixture after the permeability test (Figure 10b) are presented. The addition of lime promotes the formation of aggregates, leading to a more open soil structure in the treated sample compared to the untreated one. Figure 10b clearly shows the existence of crystalline (needle-shaped) and amorphous gel-like pozzolanic materials (spongy aspect) spread throughout the sample, reflecting the progress of long-term reactions. The bonding action of these products enhances the stiffness of the soil-lime mixture, which is reflected by the upward trend observed in G_0.

In Figure 11, a comparison between compacted untreated soil (Figure 11a) and compacted treated SLFA mixture (Figure 11b) is shown. The treated sample exhibits an uneven distribution of pozzolanic substances. Within the SLFA mixture (Figure 11b), two distinct forms of fly ash can be observed: one type consists of reacted fly ash with a textured surface, while the other type comprises smooth, unreacted spherical particles. Due to coating by amorphous pozzolanic materials (Fraay et al., 1989; Chindaprasir et al. 2007) reacted fly ash particles shows a rough texture. On the other hand, unreacted particles act merely as a filler, enhancing the packing density of the mixture. Crystalline acicular C-S-H formations can be identified in the sample, resulting from the reaction between lime and silica present in the soil fine fraction. These crystalline formations, found in both the SL mixture and the SLFA mixture connect the walls of inter-aggregate pores, effectively bonding the soil particles and thus contributing to increased stiffness, as indicated by the outcomes of the BE test.

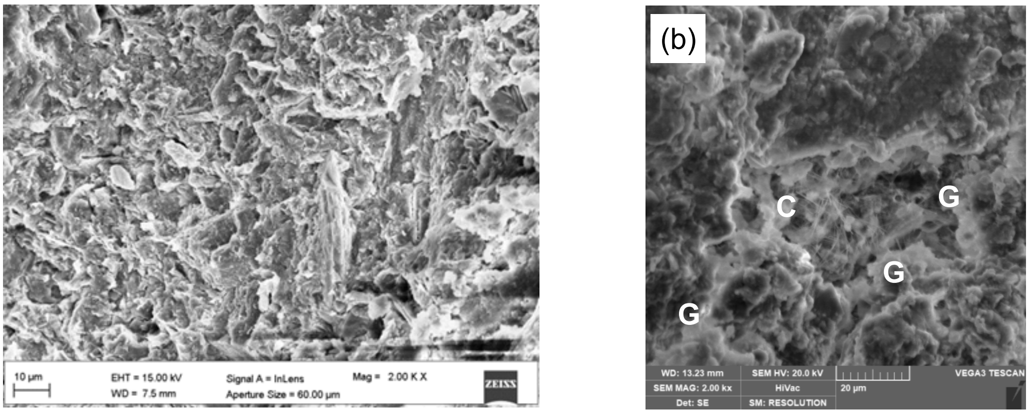

Figure 10. SEM images of (a) untreated soil (b) SL mixture at the end of permeability test (C=crystalline pozzolanic products; G=Gel-form pozzolanic products).

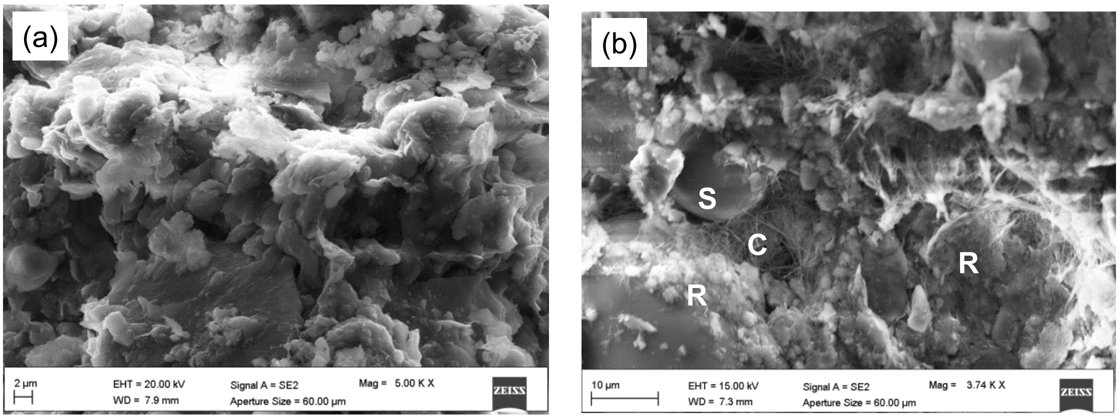

Figure 11. SEM images of (a) untreated soil (b) SLFA mixture (C=crystalline pozzolanic products; R=rough-surface FA particle; S=smooth-surface FA particle)

4.3.3 *Practical implications*

Considering the results presented in the previous sections, it is possible to state that G_0 is a promising parameter to monitor the development of cementation (i.e. pozzolanic) reactions in amended soils. The use of BE for the measurement of the small-strain stiffness, a relatively simple and cost-effective method, can reduce the number of both laboratory tests to be performed in the design phase of the mixture and the in-situ quality control tests. In fact, traditional geotechnical tests such as oedometric, triaxial or unconfined compression tests could be carried out only for those mix designs able to ensure a minimum G_0 values at specified curing times, thus avoiding the investigation of several mix design combinations. Referring to the in-situ phase, the construction quality controls can be more efficiently programmes based on the G_0 trend with curing time; in this way, economic and practical efforts can be concentrated in testing the performance of the mixture in the proper curing period.

5 CONCLUSIONS

The paper demonstrates the application of the Bender Element (BE) method to monitor the changes in the small-strain shear modulus, G_0, throughout the curing period from 0 to 90 days post-preparation in cement-bentonite, compacted soil-lime, and compacted soil-lime-fly ash mixtures, all frequently utilized in geo-environmental projects. Three distinct CB mixtures, one SL and one SLFA mixture were evaluated. The hydraulic conductivity of these geo-materials was also assessed throughout the same curing interval by means of permeability tests.

In the application of BE testing to geo-materials that display time-related properties, it is in general recommended to apply multiple frequencies, f, for the transmitted signal at a specific curing time to determine the most effective signal. To achieve accurate measurement of G_0, it was essential in this study to maintain the ratio of L_{tt} (tip-to-tip of the BE distance) to the wavelength, λ within the range $2 < Ltt/\lambda < 9$, which facilitated clear signal readability.

The results obtained indicated that the G_0 values for the CB mixtures increased as curing time progressed, while k showed a notable reduction. The quality of the bentonite and the presence of additives were the controlling factor on k of the CB mixtures, given a specific cement content. The ratio of cement to water in the CB mixtures controlled the G_0 for differing dosages utilizing the same ingredients. Furthermore, the quality and/or source of the components used in the CB mixtures significantly influenced the results, as evidenced by the considerable difference in G_0 values for CB mixtures of identical age and comparably similar compositions reported in this study and existing literature. The small-strain shear modulus for SL and SLFA mixtures exhibited an increase with curing duration, a trend linked to the chemical interactions of soil and lime and the resultant formation of hydration products, which was corroborated by post-test SEM imaging conducted on the specimens. The trend of hydraulic conductivity of SL and SLFA mixtures displayed a similar pattern (immediate increase with respect to the untreated soil due to cation exchange-induced flocculation, followed by moderate reduction with time) which can be ascribed to the same processes (formation of cementitious products) that led to the increase in G_0.

ACKNOWLEDGEMENTS

Financial support for this work was provided by Università Politecnica delle Marche (Italy) under Grant PSA (Progetto Strategico di Ateneo) Call 2017.

REFERENCES

Arroyo M, Muir Wood D, Greening PD (2003). Source near-field effects and pulse tests in soil samples. Geotéchnique, 53(3),337–45.

Arulnathan R, Boulanger RW, Riemer MF (1998). Analysis of bender element tests. ASTM Geotechnical Testing Journal; 21(2):120–31.

ASTM C232 (2021). Standard Test Methods for Bleeding of Concrete. ASTM International, West Conshohocken, PA, USA.

ASTM D422 (2014). Standard Test Methods for Particle -Size Analysis of Soils. ASTM International, West Conshohocken, PA, USA.

ASTM D2487 (2017). Standard Practice for Classification of Soils for Engineering Purposes (Unified Soil Classification System). ASTM International, West Conshohocken, PA, USA.

ASTM D8295 (2019). Standard Test Methods for Determination of Shear Wave Velocity and Initial Shear Modulus in Soil Specimens using Bender Elements. ASTM International, West Conshohocken, PA, USA.

ASTM D698 (2021). Standard Test Methods for Laboratory Compaction Characteristics of Soil Using Standard Effort. ASTM International, West Conshohocken, PA, USA.

Beetham P, Dijkstra T, Dixon N, Fleming P, Hutchinson R, Bateman J (2014). Lime stabilisation for earthworks: a UK perspective. Proc. Inst. Civ. Eng.–Ground Improvement, 168 (GI2), 81-95.

Bellezza I, Fratalocchi E (2006). Effectiveness of cement on hydraulic conductivity of compacted soil–cement mixtures. Proc. Inst. Civ. Eng Ground Improvement, 10(2), pp. 77–90.

Chindaprasirt P, Jaturapitakkul C, Sinsiri T (2007). Effect of fly ash fineness on microstructure of blended cement paste. Constr. and Build. Mat. 21, 1534–1541

Costa LT, Vitale E, Cappelletti P, Graziano SF, Rispoli C, Russo G (2023). Alkaline activation of volcanic ash as binder for soil improvement. Proceedings of the 8th Italian Conference of researchers in Geotechnical Engineering, Ferrari, Rosone, Ziccarelli, Gottardi (eds.), Springer, 792-799. https://doi.org/10.1007/978-3-031-34761-0_95

Devi K, Chachia A, Kumar A (2020). Soil Improvement Using Waste Materials: A Review. Journal of Building Material Science 02(01), 11-17; https://doi.org/10.30564/jbms.v2i1.2641

Di Sante M, Bernardo D, Bellezza I, Fratalocchi E, Mazzieri F (2022). Linking small-strain stiffness to development of chemical reactions in lime-treated soils. Transportation Geotechnics, v.34, 100742 .1-7 (doi: 1 0.1016/j.trgeo.2022.100742)

Di Sante M, Di Buò B, Fratalocchi E, Länsivaara T (2020). Lime treatment of a soft sensitive clay: A sustainable reuse option. Geosciences, 2020, 10(5), 182.

Dyvick R, Madshus C (1985). Lab measurements of Gmax using bender elements. Advances in the Art of Testing Soils under Cyclic Conditions. New York: ASCE, 1985:186—196.

Fraay A, Bijen JM, de Haan YM (1989). The reaction of fly ash in concrete: A critical examination. Cement Concrete Research 19, 235–46.

Fratalocchi E, Pasqualini E (1998). Permeability over time of cement -bentonite slurry walls. Proceedings of the 3rd International Congress on Environmental Geotechnics, ICEG. Lisbon, pp. 509-514.

Fratalocchi E, Brianzoni V, Di Sante M, Mazzieri F, Pasqualini E (2013). Migration of aggressive solutions through CB walls. Proc. 1st Int. Symposium on Coupled Phenomena in Environmental Geotechnics, CPEG2013, Turin (Italy), Taylor and Francis, 243-252.

Fratalocchi E, Felici M, Domizi J; Mazzieri F (2022). "Recenti sviluppi nello studio delle prestazioni dei diaframmi plastici". Proceedings XVII National Congres, Reggio Calabria, Italy 13-15 Luglio 2022, pp. 321-337 (in Italian)

ICE, Institution of Civil Engineers, CIRIA, Construction Industry Research and Information Association, BRE, Building Research Establishment (1999). Specification for the construction of slurry trench cut-off walls as barriers to pollution migration. Thomas Telford, London.

Ingale R, Patel A, Mandal A (2019). A study on dynamic small-strain shear modulus of fly ash stabilized expansive soil. Proceedings of Indian geotechnical Conference.

Jefferis SA(1981). Bentonite-cement slurries for hydraulic cutoffs. Proc. X ICSMFE, Vol. 1, 435-440.

Kang X (2015). Mechanical characteristics of organically modified fly ash-kaolinite mixtures. Ph.D. Dissertation, Missouri University of science and Technology, Rolla, MO, USA.

Lee JS, Santamarina JC (2005). Bender elements: Performance and signal interpretation. Journal of Geotechnicaal and Geoenvironmental Engineering, ASCE 2005;131(9):1063–70. https://doi.org/10.1061/ASCE 1090-0241(2005)131:9(1063)).

Li Y， Yang J， Lan J， Huang C (2019). Experimental study on age effect and influence factor of slag-cement-bentonite's shear modulus. Journal of Hunan University（Natural Sciences. 46(9). DOI:10.16339/j.cnki.hdxbzkb.2019.09.015 (in Chinese).

Liu H, Cascante G, Maghoul P, Shalaby A (2021). Experimental investigation and numerical modelling of piezoelectric bender element motion and wave propagation analysis in soils. Canadian Geotecnical Journal, 59(3).

Noaman MF, Khan MA, Ali K, Hassan A (2022). A review on the effect of fly ash on the geotechnical properties and stability of soil. Cleaner Materials 6, 1001551. https://doi.org/10.1016/j.clema.2022.100151

Petcherdchoo S, Pochalar K, Piriyakul K (2023). Use of bender element tests for determining shear modulus of fly-ash and cement admixed Bangkok clay with considering unconfined compressive strength. Case Studies in Construction Materials

18, e02040 https://doi.org/10.1016/j.cscm.2023.e02040

Piriyakul K (2014). Using Shear Wave Velocity to Assess the Stiffness of Soil-Cement-Fly Ash. Applied Mechanics and Materials 459, 115-118. https://doi.org/10.4028/www.scientific.net/AMM.459.115

Puppala AJ, Intharasombat N, Vempati R K (2005). Experimental studies on ettringite-induced heaving in soils. Journal of Geotechnical and Geoenvironmental Engineering, 131(3), 325-337.

Puppala AJ, Bhadriraju V, Madhyannapu RS, Hoyos, LR (2006). Small strain shear moduli of chemically stabilized sulfate-bearing cohesive soils. J. Geotech. Geoenv. Eng. ASCE 132, No. 3, 322-336 http://dx.doi.org/10.1061/(ASCE)1090-0241(2006)132:3(322))

Puppala A, Manosuthiki J, Chittoori B (2013). Swell and shrinkage characterizations of unsaturated expansive clays from Texas. Engineering Geology, 164(3), 187-194.

Ram AK, Mohanty S (2021). Experimental investigation on dynamic behavior of silt−rich fly ash using cyclic triaxial and bender element tests. Innovative Infrastructure Solutions 6, 219. https://doi.org/10.1007/s41062-021-00582-1.

Sanchez Salinero I, Rosset JM , Stokoe, K.H.II (1986). Analytical studies of body wave propagation and attenuation. Rep.n. GR-86-15, Univ. of Texas, Austin, TX.

Tang AM, Vu MN, Cui YJ (2011). Effects of the maximum soil aggregates size and cyclic wetting-drying on the stiffness of a lime-treated clayey soil. Géotechnique 61(5), 421-429.

Transportation Research Board (1987). "State of the art report 5: Lime stabilization – Reactions, properties, design and construction", Washington.

UNI EN 459-1 (2010). La nuova classificazione delle calci idrauliche. (in Italian)

Verástegui Flores RD, Di Emidio G (2013). Hydraulic conductivity and small-strain stiffness of a cement-bentonite sample exposed to sulphates. Proceedings of the 18th International Conference on Soil Mechanics and Geotechnical Engineering, Paris 2013, 977-980.

Verástegui Flores RD, Di Emidio G, Van Impe W (2010). Small strain shear modulus and strength increase of cement-treated clay. Geotechnical Testing Journal 33(1), 62–71

Wang YH, Lo KF, Yan WM, Dong XB (2007). Measurement biases in the bender element test. Journal of Geotechnical and Geoenvironmental Engineering. ASCE;133(5):564–74. https://doi.org/10.1061/(ASCE) 1090-0241(2007)133:5(564)).

Wang Y, Benahmed N, Tang AM (2017). A novel method for determining the small-strain shear modulus of soil using the bender elements technique. Canadian Geotechnical Journal. 54(2), 280-289.

Wang Y, Cui YJ, Benahmed N, Tang AM, Duc M (2020). Changes of small strain shear modulus and suction for a lime-treated silt during curing. Géotechnique, 70(3), 276-280.

Wild S, Arabi M, Rowlands GO (1987). Relation between pore size distribution, permeability and cementious gel formation in cured clay-lime systems. Material Science and Technology 3(12), 1005-1011.

Winterkorn HF, Pamukcu S (1991). Soil stabilization and grouting. Foundation Engineering Handbook. Hsai-Yang Fang ed., Van Nostrand Reinhold, New York, 317-378

List of figure captions

Figure 1. SEM images of the FA (Magnification:1000x)

Figure 2. Examples or transmitted and received signals during BE testing of CB mixtures.

Figure 3. G_0 versus curing time for the CB mixtures investigated. Dashed lines are the best-fit curves of experimental data for CB 1 and CB 2

Figure 4. Hydraulic conductivity vs. curing time of the three CB mixtures investigated. Dashed lines are the best fit curve of experimental data according to Equation2.

Figure 5. G_0 vs. curing time for the SL mixture investigated.

Figure 6. **G_0 vs. curing time for the SLFA mixture investigated**.

Figure 7 Resonant frequency f_R of the SL and SLFA specimens as a function of curing time

Figure 8. Hydraulic conductivity versus curing time for the SL mixtures investigated. The hydraulic conductivity of the compacted untreated soil is shown for comparison.

Figure 9. Hydraulic conductivity versus curing time for the SLFA mixtures investigated. The hydraulic conductivity of the compacted untreated soil is shown for comparison.

Figure 10. SEM images of (a) untreated soil (b) SL mixture at the end of permeability test (C=crystalline pozzolanic products; G=Gel-form pozzolanic products).

Figure 11. SEM images of (a) untreated soil (b) SLFA mixture (C=crystalline pozzolanic products;R=rough-surface FA particle; S=smooth-surface FA particle

LIST OF TABLE CAPTIONS

Table 1 Main properties of the soils used in this study

Table 2. Main physical properties of the tested CB mixtures